Biochimica et Biophysica Acta 1828 (2013) 1374–1383

Contents lists available at SciVerse ScienceDirect

Biochimica et Biophysica Acta

journal homepage: www.elsevier.com/locate/bbamem

Alternative cycling modes of the Na^+/K^+-ATPase in the presence of either Na^+ or Rb^+☆

José L.E. Monti *, Mónica R. Montes, Rolando C. Rossi

Instituto de Química y Fisicoquímica Biológicas and Departamento de Química Biológica, Facultad de Farmacia y Bioquímica, Universidad de Buenos Aires, Junín 956, 1113 Buenos Aires, Argentina

ARTICLE INFO

Article history:
Received 1 September 2012
Received in revised form 10 January 2013
Accepted 15 January 2013
Available online 25 January 2013

Keywords:
Na^+/K^+-ATPase
Steady-state kinetics
Phosphoenzyme
Rb^+-occlusion
ATPase activity
Minimal model

ABSTRACT

A comprehensive study of the interaction between Na^+ and K^+ with the Na^+/K^+-ATPase requires dissecting the incidence of alternative cycling modes on activity measurements in which one or both of these cations are absent. With this aim, we used membrane fragments containing pig-kidney Na^+/K^+-ATPase to perform measurements, at 25 °C and pH = 7.4, of ATPase activity and steady-state levels of (i) intermediates containing occluded Rb^+ at different [Rb^+] in media lacking Na^+, and (ii) phosphorylated intermediates at different [Na^+] in media lacking Rb^+. Most relevant results are: (1) Rb^+ can be occluded through an ATPasic cycling mode that takes place in the absence of Na^+ ions, (2) the kinetic behavior of the phosphoenzyme formed by ATP in the absence of Na^+ is different from the one that is formed with Na^+, and (3) binding of Na^+ to transport sites during catalysis is not at random unless rapid equilibrium holds.

1. Introduction

Na^+/K^+-ATPase (or sodium pump) is a transmembrane protein [1,2] present in the plasma membrane of eukaryotic cells [3–5]. Under physiological conditions, this enzyme couples the hydrolysis of one intracellular ATP molecule (into ADP and orthophosphate) to the exchange of three intracellular Na^+ (Na^+_i) for two extracellular K^+ (K^+_e), being intracellular Mg^{2+} an essential activator for the reaction. During the catalytic cycle the enzyme undergoes phosphorylation and dephosphorylation and the transported cations become transitorily occluded (trapped within the enzyme). K^+-occluded intermediates can be obtained either through the *direct route*, without formation of phosphoenzyme, or through the *physiological route*, after K^+-stimulated dephosphorylation of the phosphoenzyme. A scheme for the catalytic cycle under physiological conditions, based on the currently accepted Albers–Post model [4,5], is given in Fig. 1.

Under non-physiological conditions, alternative cycling modes have also been reported [6–15]. These studies showed that ATP hydrolysis can be coupled to the exchange of Na^+_i for Na^+_e, Na^+_i for H^+_e and H^+_i for K^+_e.

The global functioning of the enzyme can be evaluated by steady-state determinations of the rate of reactants consumption/generation and this evaluation is better supported by including parallel determinations of the concentration of enzyme reaction intermediates. Steady-state kinetics does not always follow the classic Michaelis–Menten behavior (rectangular hyperbola) as a certain reactant (substrate or product) concentration is varied. In fact, non-michaelian kinetics is obtained when: 1) such reactant binds to more than one reaction intermediate within the catalytic cycle and/or 2) alternative catalytic pathways coexist under the conditions tested. Both statements apply to Na^+/K^+-ATPase giving non-hyperbolic curves when varying the concentration of the transported cations. Due to the poor development of theoretical tools for the analysis of these complex curves, most of the details about the catalytic mechanism of the pump have been obtained from the analysis of transient-state kinetics. Although transient-state kinetics provides very valuable information, it evaluates only partial reactions, not the global functioning of the enzyme.

This work is part of a more extensive study of the global functioning of the pump, which is aimed at validating the ping-pong nature of the transport of Na^+ and K^+. We have here characterized and modeled alternative cycling modes from the analysis of steady-state determinations of ATPase activity and intermediates phosphorylated or occluded with Rb^+ (a K^+ analogue), performed in the absence of one or both of the transported cations. Although this analysis was intended to evaluate the incidence of alternative cycling modes on the kinetics of the interaction between Na^+ and Rb^+, it is worth mentioning that alternative cycling modes have an interest *per se*.

We have been able to extract information about the catalytic mechanism from the analysis of the empirical equations that best describe the results. This analysis is based on algorithms traditionally

☆ JLEM is fellow of Agencia Nacional de Promoción Científica y Tecnológica, MRM and RCR are established investigators from Consejo Nacional de Investigaciones Científicas y Técnicas.

* Corresponding author. Tel.: +54 11 4964 5506; fax: +54 11 4962 5457.
E-mail address: litomonti@gmail.com (J.L.E. Monti).

0005-2736/$ – see front matter © 2013 Elsevier B.V. All rights reserved.
http://dx.doi.org/10.1016/j.bbamem.2013.01.010

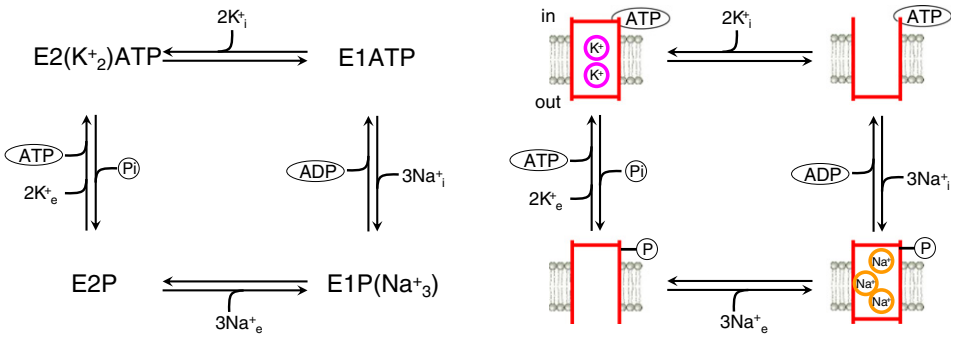

Fig. 1. A simplified version of the Albers–Post model for the physiological functioning of the sodium pump. The reaction scheme (left) has been cartooned (right) for better comprehension. Subscripts *i* and *e* are for *intracellular* and *extracellular* respectively. For the left diagram, occluded cations are written within parentheses. For the right diagram, each intermediate is represented with its cytoplasmic side ("in") facing up.

used for solving reaction models [16,17] and on methods that can be employed for simplifying models [18,19]. The most outstanding findings are: 1) Rb^+ can be occluded through an ATPasic cycling mode that takes place in the absence of Na^+ ions; 2) the kinetic behavior of the phosphoenzyme formed by ATP in the absence of Na^+ is different from the one that is formed with Na^+; 3) binding of Na^+ to transport sites during catalysis is not at random unless rapid-equilibrium holds.

2. Materials and methods

2.1. Enzyme

A purified preparation of Na^+/K^+-ATPase obtained from pig kidney red-outer medulla by treatment of the microsomal fraction with sodium dodecyl sulfate and extensive washing [20], was kindly provided by the Department of Biophysics, University of Århus, Denmark.

Enzyme (hereafter abbreviated as Ez when present in the units) was quantified by measuring occluded Rb^+ under thermodynamic equilibrium in media containing 250 μM [^{86}Rb]RbCl, 0.25 mM EDTA and 25 mM imidazole-HCl (pH = 7.4 at 25 °C). Under this condition, nearly all enzyme molecules are occluding two Rb^+. Determinations made in four independent experiments gave an average value of 2.51 ± 0.09 nmol of Ez/mg protein.

2.2. Reagents and reaction conditions

[^{86}Rb]RbCl and [γ-^{32}P]ATP were from PerkinElmer Life Sciences. All other reagents were of analytical grade.

Experiments were performed at 25 °C in media containing 2.5 mM ATP (except for phosphoenzyme determinations where 20 μM ATP was used), 0.25 mM EDTA, enough $MgCl_2$ to give 0.5 mM free Mg^{2+} (when present), 25 mM imidazole-HCl (pH = 7.4 at 25 °C), and different concentrations of RbCl (instead of KCl), NaCl, and CholineCl so that the total concentration of the last three salts was always 170 mM.

2.3. ATPase activity

ATPase activity was obtained from the time course of the release of [^{32}P]Pi from [γ-^{32}P]ATP, as described in Schwarzbaum et al. [21]. Briefly, after the incubation time, the reaction is quenched, the [^{32}P]Pi is extracted, and radiation due to Čerenkov effect is measured in a scintillation counter. Blank values were lowered by sodium citrate treatment.

The experimental procedure was as follows. In order to stop the enzyme-catalyzed ATP hydrolysis, 200 μl of the reaction media were diluted under continuous vortex mixing with 2 ml of a solution containing 0.5% P/V ammonium heptamolybdate in 0.83 M $HClO_4$. Immediately after, 2 ml of isobutanol was added in order to extract the phosphomolybdic complex completely (leaving ATP in the aqueous phase). 30 s after the reaction was stopped, and under continuous vortex stirring, 1 ml sodium citrate 2 % P/V was added and the tube was vortexed for 10 more seconds. Citrate prevents the extraction of the Pi that can be formed by chemical hydrolysis of ATP after the enzyme-catalyzed reaction is stopped. The turbidity that appeared in the organic phase after 3–5 min due to a slow phase separation was eliminated by centrifugation (2000 *g* for 10 s) and 1 ml of the organic phase was transferred to a vial and mixed with 2 ml of 0.5 M NaOH with the aim of dissociating the phosphomolybdic complex and extract the Pi into the aqueous phase.

Although hydrolysis of more than 10% of the ATP was avoided, linearity of released Pi with time was always checked in order to ensure initial rate conditions. Steady-state determinations were made in media containing a protein concentration of 20 μg/ml and incubation times ranging from zero to 30 min.

ATP hydrolysis by ATPases other than Na^+/K^+-ATPase was evaluated (and subtracted to all activity determinations) by following time courses of released Pi in media containing 170 mM K^+, giving values not significantly different from the ones obtained at 170 mM Na^+ and 1 mM ouabain.

2.4. Occluded Rb^+

The methodology employed is described in Rossi et al. [22]. Briefly, reactions were started and incubated using a rapid-mixing apparatus (SFM4 from Bio-Logic, France) and the reaction medium was squirted (at 2.5 ml/s) into a quenching-and-washing chamber. There, the reactions were stopped by sudden dilution and cooling with an ice-cold solution of 30 mM KCl in 5 mM imidazole-HCl (pH = 7.4 at 0 °C) that was flowing (at 40 ml/s) through a Millipore-type filter, where the enzyme was retained and washed.

Unspecific [^{86}Rb]Rb^+ binding to the filter was evaluated by omitting the enzyme from the reaction medium. Their values were similar to those obtained in the presence of enzyme inactivated either by heat (30 min at 65 °C) or by dilution (1/44 in 25 mM imidazole-HCl with 0.25 mM EDTA, pH = 7.4 at 25 °C) and exposure to a freeze (− 18 °C, overnight) and thaw cycle.

Steady-state determinations were made in media containing a protein concentration of 30-40 μg/ml, after an incubation time of 7 s.

2.5. Phosphoenzyme levels

The phosphorylated intermediates (EP), were measured as the amount of acid-stable ^{32}P-labeled enzyme formed during [γ-^{32}P]ATP hydrolysis. The procedure was similar to the one employed for occluded

Rb^+ determinations but the reaction was stopped with an ice-cold solution containing 7% trichloroacetic acid flowing at 17 ml/s.

Unspecific [^{32}P]Pi and [γ-^{32}P]ATP binding was evaluated by omitting Mg^{2+} in the reaction medium.

2.6. Data analysis

Empirical equations of the form:

$$f(x) = \frac{\varphi_0 + \varphi_1 \frac{x}{K_1} + \ldots + \varphi_i \frac{x^i}{K_1 K_2 \ldots K_i} + \ldots + \varphi_n \frac{x^n}{K_1 K_2 \ldots K_i \ldots K_n}}{1 + \frac{x}{K_1} + \ldots + \frac{x^i}{K_1 K_2 \ldots K_i} + \ldots + \frac{x^d}{K_1 K_2 \ldots K_i \ldots K_d}} \quad (1)$$

were fitted to the data of ATPase activity (v) and steady state concentrations of occluded Rb^+ (Occ) and of phosphorylated enzyme (EP), by weighted nonlinear regression based on the Gauss-Newton algorithm using commercial programs (Excel, Sigma-Plot, and Mathematica for Windows). In Eq. (1), x is the concentration of the tested ligand, φ_i's are coefficients with units corresponding to $f(x)$, and K_i's are apparent dissociation constants expressed in concentration units.

A systematic search of the equation that best fits each set of results was carried out, first by determining the degree of the polynomials in the numerator and the denominator of Eq. (1) and then by evaluating the contribution of terms of intermediate degree. The evaluation included fixing some coefficients' values to zero or establishing mathematical restrictions between two or more coefficients.

The goodness of fit of a given equation to the experimental results was evaluated by the corrected asymptotic information criterion [23] defined as:

$$AICc = nd \cdot \ln\left(\frac{SSr}{nd}\right) + \frac{2 \cdot (np+1) \cdot nd}{(nd - np - 2)} \quad (2)$$

where nd is the number of data points, np is the number of parameters to be fitted, and SSr is the sum of weighted square residual errors. Weighting factors were calculated as the reciprocal of the variance of experimental data.

The *AICc* criterion is based on the *information theory* (a branch of applied mathematics that provides the basis for quantifying the information), and selects among various possible equations that which gives the minimum value of *AICc*, on the basis of its capacity to explain the results using a minimal number of parameters.

3. Results and discussion

We studied both, the effect of Na^+ in the absence of Rb^+ and the effect of Rb^+ in the absence of Na^+, on the steady-state catalytic properties of Na^+/K^+-ATPase at saturating ATP concentrations. The empirical equations that best describe the results were analyzed in order to unveil critical aspects of the kinetic mechanism of the enzyme.

3.1. Parallel measurements of ATPase activity and steady-state levels of occluded Rb^+ as a function of [Rb^+] in Na^+-free media

Fig. 2 shows the dependence of ATPase activity and steady-state levels of occluded Rb^+ on [Rb^+], in media lacking Na^+. The continuous lines are the plots of equations for ATPase activity, v, and for occluded Rb^+, Occ, using the best fitting parameters values given in Table 1. Equations are:

$$v\left(\left[Rb^+\right]\right) = \frac{a_{Rb0} + a_{Rb1} \cdot \frac{[Rb^+]}{K_{Rb1}} + a_{Rb2} \cdot \frac{[Rb^+]^2}{K_{Rb1} \cdot K_{Rb2}}}{1 + \frac{[Rb^+]}{K_{Rb1}} + \frac{[Rb^+]^2}{K_{Rb1} \cdot K_{Rb2}} + \frac{[Rb^+]^3}{K_{Rb1} \cdot K_{Rb2} \cdot K_{Rb3}}} \quad (3)$$

$$Occ\left(\left[Rb^+\right]\right) = \frac{o_{Rb1} \cdot \frac{[Rb^+]}{K_{Rb1}} + o_{Rb2} \cdot \frac{[Rb^+]^2}{K_{Rb1} \cdot K_{Rb2}} + o_{Rb3} \cdot \frac{[Rb^+]^3}{K_{Rb1} \cdot K_{Rb2} \cdot K_{Rb3}}}{1 + \frac{[Rb^+]}{K_{Rb1}} + \frac{[Rb^+]^2}{K_{Rb1} \cdot K_{Rb2}} + \frac{[Rb^+]^3}{K_{Rb1} \cdot K_{Rb2} \cdot K_{Rb3}}} \quad (4)$$

where the a_{Rbi}'s and o_{Rbi}'s are coefficients with units of activity and occluded Rb^+ concentration, respectively, and K_{Rbi}'s are apparent dissociation constants expressed in mM. It is important to note that the measurements of ATPase activity and steady-state levels of occluded Rb^+ are adequately described by rational equations having the same denominator, as expected if both determinations express the steady-state behavior of the same enzyme mechanism (see for instance [24]).

ATPase activity increases ($K_{1/2} \cong 0.004$ mM) and then decreases ($K_{1/2} \cong 3$ mM) with [Rb^+] (Fig. 2A). It can be seen in Fig. 2B, that there is a significant amount of ouabain-sensitive ATPase activity in the absence of Rb^+, represented by the parameter a_{Rb0} in Eq. (2), indicating that neither Na^+ nor Rb^+ are necessary for ATP hydrolysis as found in previous studies [7,9,10]. In media lacking both Na^+ and Rb^+, enzyme's operating mode will be called the *X/X-ATPasic cycling mode* as it is not clear whether the enzyme does not transport cations or if it transports other cations present in the medium, being H^+ a

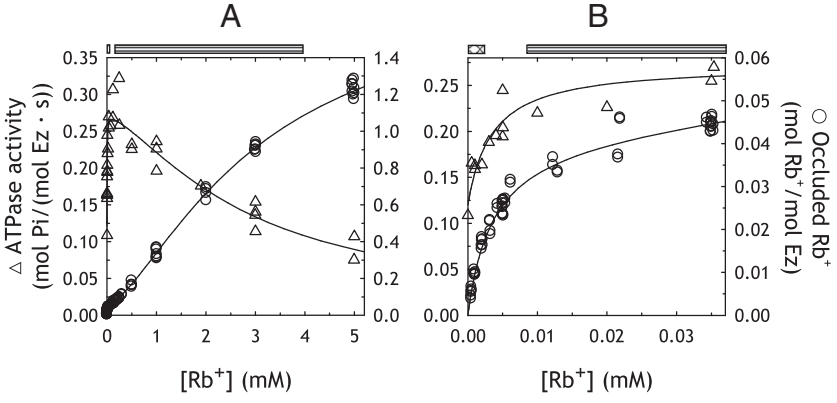

Fig. 2. Dependence of ATPase activity (△) and steady-state levels of occluded Rb^+ (○) on [Rb^+] when Na^+ is absent. Media contained 2.5 mM ATP, 0.5 mM free Mg^{2+}, 0.25 mM EDTA, 25 mM imidazole-HCl and different concentrations of RbCl and CholineCl, being the total concentration of the last two salts equal to 170 mM. Panel B shows a detail of the results obtained up to 0.035 mM Rb^+. The continuous lines are plots of the empirical Eqs. (3) and (4) for the best global fitting values of their parameters (see Table 1). The predominant cycling mode is indicated at the top of each chart: X/X-ATPasic (▭) and X/Rb^+-ATPasic (═) modes.

Table 1
Best global fitting values of the parameters present in Eqs. (3) and (4) to the results shown in Fig. 2.

Parameter	Value ± SE	Units
o_{Rb1}	0.04262 ± 0.00081	mol Rb^+/mol Ez
o_{Rb2}	0.51 ± 0.17	mol Rb^+/mol Ez
o_{Rb3}	1.90 ± 0.13	mol Rb^+/mol Ez
K_{Rb1}	0.00352 ± 0.00014	mM
K_{Rb2}	2.63 ± 0.83	mM
K_{Rb3}	2.54 ± 0.52	mM
a_{Rb0}	0.120 ± 0.017	mol Pi/(mol Ez · s)
a_{Rb1}	0.275 ± 0.014	mol Pi/(mol Ez · s)
a_{Rb2}	0.168 ± 0.039	mol Pi/(mol Ez · s)

Table 2
Best fitting values of the parameters present in Eq. (5). Parameters $o_{Rb1,\ Mg=0}$ and $o_{Rb2,\ Mg=0}$ were fixed to 1 and 2 respectively because studies on occlusion of Rb^+ through the direct route [29] show that all enzyme species with occluded Rb^+ (one or two cations) are detected and all the species with bound (and not occluded) Rb^+ are negligible.

Parameter	Value ± SE	Units
$o_{Rb1,\ Mg=0}$	1	mol Rb^+/mol Ez
$o_{Rb2,\ Mg=0}$	2	mol Rb^+/mol Ez
$K_{Rb1,\ Mg=0}$	1.474 ± 0.095	mM
$K_{Rb2,\ Mg=0}$	0.452 ± 0.079	mM

possible candidate [11,13–15]. Structural basis for the binding of H^+ to the transport sites, both from the cytoplasmic side [25] and from the extracellular side [26] were recently found through the analysis of the crystal structure of the Na^+/K^+-ATPase.

The steady-state level of occluded Rb^+ increases with the concentration of the cation along a curve that can be described as the sum of two components, one hyperbolic and the other sigmoid. The hyperbolic component (better seen on panel B of Fig. 2) has high affinity ($K_{1/2} \cong 0.004$ mM) and small amplitude (about 2% of the value of occluded Rb^+ when $[Rb^+]$ tends to infinity), and is correlated with the increase in ATPase activity. On the other hand, the sigmoid component has low affinity ($K_{1/2} \cong 3$ mM) and large amplitude (around 2 mol Rb^+/mol Ez, i.e. the maximum value for occluded Rb^+), and is correlated with the decrease in ATPase activity. The sigmoid component is likely due to the occlusion of Rb^+ through the direct route since, if Rb^+ competes by binding to the enzyme available for phosphorylation, ATPase activity should decrease.

Nevertheless, as occluded-Rb^+ species mediate the transport of Rb^+ [27,28], the correlation between the hyperbolic component of occluded Rb^+ and the increase in ATPase activity seen at low Rb^+ concentrations (Fig. 2B), suggests that the enzyme is transporting Rb^+ even in the absence of Na^+. This would be related to a cycling mode similar to the physiological one, which can be called the *X/Rb⁺-ATPasic cycling mode*, where Na^+ ions are replaced by some other cations, including Rb^+ as a possible candidate. This interpretation is reinforced by the fact that when Mg^{2+} (an essential cofactor for the enzymatic hydrolysis of ATP) is omitted from the reaction media this hyperbolic component disappears (Fig. 3), and Rb^+ occlusion takes place only through the direct route.

It is worth to mention that the sigmoidal component of occluded Rb^+ observed after the completion of the hyperbolic one starts with a slope that is significantly lower than that obtained in the absence of Mg^{2+} (Fig. 3A). This agrees with results obtained in equilibrium indicating that despite one Mg^{2+} and one Rb^+ ions can be simultaneously bound to the enzyme, this Rb^+ cannot become occluded [29]. In contrast, in the absence of Mg^{2+} a nonzero slope is observed at low $[Rb^+]$ (filled circles in Fig. 3B) which is explained by the occlusion of one cation. Besides, as the curve of Rb_{occ} vs. $[Rb^+]$ obtained in the presence of Mg^{2+} can reach the maximum possible level of 2 Rb^+ per enzyme unit (see Table 1), and that for $[Rb^+]$ above 0.1 mM the values of results obtained in the absence of Mg^{2+} are greater than in its presence (Fig. 3A) it can be concluded that the apparent affinity for Rb^+ is higher in the absence of the divalent cation. This also agrees with previous studies of the direct route of occlusion showing that Mg^{2+} is displaced from the enzyme in a competitive manner by the binding (and the subsequent occlusion) of a second Rb^+ ion [29].

The following empirical equation adequately describes the results obtained when Mg^{2+} is omitted from the reaction media (parameters values are given in Table 2):

$$Occ_{Mg=0}\left(\left[Rb^+\right]\right) = \frac{o_{Rb1,Mg=0}\cdot\frac{[Rb^+]}{K_{Rb1,Mg=0}} + o_{Rb2,Mg=0}\cdot\frac{[Rb^+]^2}{K_{Rb1,Mg=0}\cdot K_{Rb2,Mg=0}}}{1+\frac{[Rb^+]}{K_{Rb1,Mg=0}}+\frac{[Rb^+]^2}{K_{Rb1,Mg=0}\cdot K_{Rb2,Mg=0}}} \quad (5)$$

Unlike Eq. (4), Eq. (5) is a second-order rational function of $[Rb^+]$, which is consistent with the binding and occlusion of one or two Rb^+ ions that, due to the absence of Mg^{2+}, has to occur in equilibrium conditions.

The results described above demonstrate that there is occlusion of Rb^+ due to a cycling mode that takes place in the absence of Na^+.

3.2. Parallel measurements of ATPase activity and steady-state levels of phosphoenzyme as a function of $[Na^+]$ in Rb^+-free media

Fig. 4 shows the dependence of ATPase activity and steady-state levels of phosphoenzyme (EP) on $[Na^+]$, in media lacking congeners of K^+.

ATPase activity decreases ($K_{1/2} \cong 0.2$ mM) and then increases continuously with $[Na^+]$, without showing signs of saturation at the maximum $[Na^+]$ tested. EP steady-state levels start from a nonzero value and exhibit a high affinity ($K_{1/2} \cong 0.3$ mM) sigmoid increase with $[Na^+]$, which is followed by a low affinity decrease. It is worth mentioning that despite EP determinations were performed at 0.02 mM ATP while 2.5 mM were employed in ATPase activity measurements, results should be comparable since in the absence of K^+ the K_M for the hyperbolic increase in EP levels with [ATP] equals 0.16 μM [21,30,31].

It should be stressed that in media lacking both Na^+ and Rb^+, enzyme phosphorylation depends strongly on the buffer composition. It has been previously shown by Schuurmans Stekhoven et al. [32] that increasing concentrations of imidazole-H^+ lead to higher EP levels.

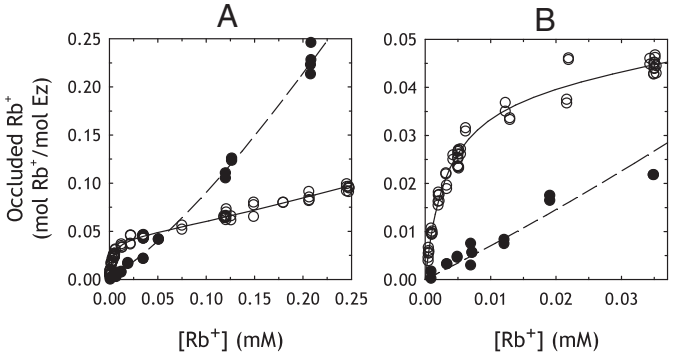

Fig. 3. Effect of omitting Mg^{2+} on occluded Rb^+ levels. Media composition is the same as the one described in Fig. 2 except for the omission of Mg^{2+} (●). The results shown here for Mg^{2+}-containing media (○) are the same as those in Fig. 2. The dashed line is the plot of Eq. (5) for the parameter values that gave the best fit (see Table 2).

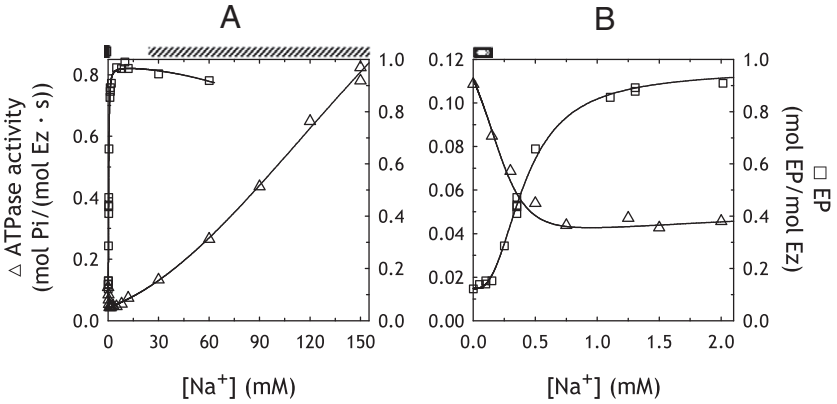

Fig. 4. Dependence of ATPase activity (△) and phosphoenzyme (EP) (□) steady-state levels on $[Na^+]$ when Rb^+ is absent. Measurements were performed in media containing 2.5 or 0.02 mM ATP for ATPase activity or EP steady-state levels, respectively, enough $MgCl_2$ to obtain 0.5 mM free Mg^{2+}, 0.25 mM EDTA, 25 mM imidazole-HCl and different concentrations of NaCl and CholineCl (being the total concentration of the last two salts equal to 170 mM). The continuous lines are plots of the empirical Eqs. (6) and (7), for the best global fitting values of their parameters (see Table 3). The predominant cycling mode is indicated at the top of each chart: X/X-ATPasic mode (▭) and Na^+/Na^+-ATPasic mode (▱).

The continuous lines shown in Fig. 4 are the plot of the following empirical equations describing ATPase activity (v) and EP levels for the parameters values given in Table 3:

$$v\left(\left[Na^+\right]\right) = \frac{a_{Na0} + a_{Na3}\cdot\frac{[Na^+]^3}{K_{Na1}\cdot K_{Na2}\cdot K_{Na3}} + \frac{+a_{Na4}\cdot\frac{[Na^+]^4}{K_{Na1}\cdot K_{Na2}\cdot K_{Na3}\cdot K_{Na4}} + a_{Na5}\cdot\frac{[Na^+]^5}{K_{Na1}\cdot K_{Na2}\cdot K_{Na3}\cdot K_{Na4}\cdot K_{Na5}}}{1+\frac{[Na^+]}{K_{Na1}}+\frac{[Na^+]^2}{K_{Na1}\cdot K_{Na2}}+\frac{[Na^+]^3}{K_{Na1}\cdot K_{Na2}\cdot K_{Na3}}+ + \frac{[Na^+]^4}{K_{Na1}\cdot K_{Na2}\cdot K_{Na3}\cdot K_{Na4}}+\frac{[Na^+]^5}{K_{Na1}\cdot K_{Na2}\cdot K_{Na3}\cdot K_{Na4}\cdot K_{Na5}}} \quad (6)$$

$$EP\left(\left[Na^+\right]\right) = \frac{e_{Na0} + e_{Na1}\cdot\frac{[Na^+]}{K_{Na1}} + e_{Na2}\cdot\frac{[Na^+]^2}{K_{Na1}\cdot K_{Na2}} + e_{Na3}\cdot\frac{[Na^+]^3}{K_{Na1}\cdot K_{Na2}\cdot K_{Na3}}}{1+\frac{[Na^+]}{K_{Na1}}+\frac{[Na^+]^2}{K_{Na1}\cdot K_{Na2}}+\frac{[Na^+]^3}{K_{Na1}\cdot K_{Na2}\cdot K_{Na3}}+ + \frac{[Na^+]^4}{K_{Na1}\cdot K_{Na2}\cdot K_{Na3}\cdot K_{Na4}}+\frac{[Na^+]^5}{K_{Na1}\cdot K_{Na2}\cdot K_{Na3}\cdot K_{Na4}\cdot K_{Na5}}} \quad (7)$$

where the a_{Nai}'s and e_{Nai}'s are coefficients with units of activity and phosphoenzyme level, respectively, and K_{Nai}'s are apparent dissociation constants expressed in mM. As before, note that ATPase activity and EP steady-state levels share the same denominator.

The small but significant amount of EP observed at null $[Na^+]$ (Fig. 4B), indicates that the X/X-ATPasic cycling mode also involves the formation of phosphorylated intermediates, and agrees with previous studies [15,32].

The decrease in ATPase activity observed when $[Na^+]$ increases from 0 to 0.2 mM is not accompanied by significant variations on EP steady-state levels (see Fig. 4B). A possible explanation for this is that Na^+ decreases the rates of both phosphorylation and dephosphorylation of the X/X-ATPasic cycling mode to a similar extent.

As shown in Fig. 4B, the increase in EP levels over the Na^+ concentration range of 0–2 mM is sigmoid and takes place at lower Na^+ concentrations than those necessary to stimulate the ATPase activity. The sigmoid increase in EP levels is consistent with the assumption that the rate of enzyme phosphorylation significantly increases only when the high-affinity transport sites for Na^+ are fully occupied. The high EP levels achieved (almost all the enzyme is phosphorylated when $[Na^+]$ ranges 2-15 mM) indicates that, under these conditions, ATPase activity is significantly limited by the *effective* rate of dephosphorylation. This does not necessarily mean that the dephosphorylation reaction is itself slow but that the low affinity for sodium of the sites in E2P does not allow the formation of significant amounts of the reactive complex.

The continuous increase in ATPase activity observed at high $[Na^+]$ shows a good correlation with the mild decrease of EP levels. This agrees with previous works showing that dephosphorylation can be promoted by Na^+ but with a much lower affinity than that for enzyme phosphorylation [33,34]. The results are also consistent with studies on Na^+ fluxes mediated by the pump [12,35], where it is shown that net hydrolysis of ATP is coupled to the exchange of Na^+_i for Na^+_e, the latter behaving like K^+_e but with much lower affinity. This operating mode of the enzyme is known as the *Na^+/Na^+-ATPasic cycling mode*.

It is of particular relevance to observe that the increase in EP levels with $[Na^+]$ over the concentration range of 0.2–2 mM lies on the term containing e_{Na3} in Eq. (7). The Albers–Post model poses that enzyme phosphorylation is greatly promoted by the simultaneous binding of three Na^+ with high affinity to intracellular transport sites in E1ATP. Under the assumption that the rapid equilibrium condition is not fulfilled, binding of Na^+ cannot occur at random, since in this case the numerator of Eq. (7) for EP would require terms with $[Na^+]$ raised to powers higher than three (see for instance [36]). The simultaneous low-affinity binding of two Na^+_e (mimicking K^+) promotes enzyme dephosphorylation, which is the rate limiting step when Rb^+ is absent [33]. The low-affinity decrease in EP levels and increase in ATPase activity with $[Na^+]$ is described by the terms containing $[Na^+]$ to the fourth and fifth powers (Eqs. (6) and (7)), i.e. not more than two powers higher than the three used in the description of enzyme phosphorylation. Therefore, the binding of Na^+ to their two extracellular transport sites cannot take place at random unless rapid equilibrium conditions are met.

In addition, our results suggest that the rate of spontaneous dephosphorylation of the phosphoenzyme formed in the absence of

Table 3
Best global fitting values of the parameters present in Eqs. (6) and (7) to the results shown in Fig. 4. The precise values for the parameters a_{Na4}, K_{Na4} and K_{Na5} cannot be determined because of the relatively high value of K_{Na4} when compared to the maximum $[Na^+]$ tested.

Parameter	Value ± SE	Units
$e_{Na0} = e_{Na1} = e_{Na2}$	0.1230 ± 0.0067	mol EP/mol Ez
e_{Na3}	0.9730 ± 0.0075	mol EP/mol Ez
$K_{Na1} = K_{Na2}$	0.78 ± 0.12	mM
K_{Na3}	0.072 ± 0.017	mM
$K_{Na5}\cdot K_{Na4}$	59,244 ± 17,539	mM^2
a_{Na0}	0.111 ± 0.019	mol Pi/(mol Ez · s)
a_{Na3}	0.0432 ± 0.0096	mol Pi/(mol Ez · s)
a_{Na4}/K_{Na4}	0.00197 ± 0.00086	mol Pi/(mol Ez · s · mM)
a_{Na5}	2.05 ± 0.47	mol Pi/(mol Ez · s)

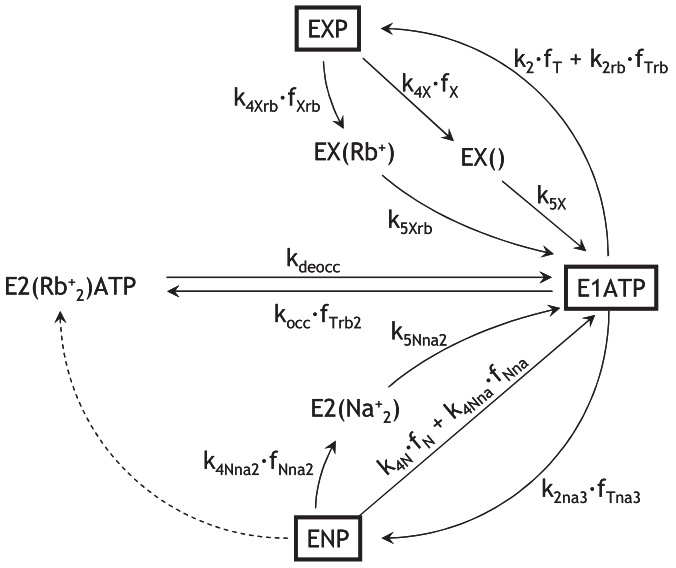

Fig. 5. A minimal model that reproduces the results. Each box represents a rapid equilibrium segment, that is, a set of reaction intermediates (shown in Fig. 6) under rapid equilibrium conditions. k's are rate constants and f's are fractional concentrations for the reaction intermediate involved in a given step (see Table 4). Intermediates corresponding exclusively to the X/X-ATPase cycle (upper part of the scheme) are the phosphoenzyme EXP and the dephosphoforms EX, while the normal phosphoenzyme formed in Na^+-containing media (lower part of the scheme) is denoted ENP. Occluded cations are shown between parentheses, and equilibrium segments E1ATP, ENP and EXP (displayed in detail in Fig. 6) are included in "boxes". The dashed arrow represents a reaction step that belongs to the Na^+/Rb^+-ATPasic cycling mode and was not considered because sodium and rubidium were never simultaneously present under the conditions tested.

Na^+ is higher than that for the phosphoenzyme formed with Na^+. This can be inferred from the fact that dephosphorylation is an irreversible reaction (due to the absence of Pi) and therefore the ATPase activity should equal the product between EP and the apparent rate constant of dephosphorylation, i.e. $v = EP \times k_{dephos}$. When Na^+ is absent, v is 0.10 mol Pi/(mol Ez · s) and EP is 0.13 mol EP/mol Ez, and therefore $k_{dephos,[Na^+]=0}$ is 0.77 s^{-1}. On the other hand, when $[Na^+]$ is 2 mM, we can assume that almost all EP present is formed upon the simultaneous binding of three Na^+ to E1ATP and that ATPase activity is mainly limited by the rate of spontaneous dephosphorylation. Under this condition, v is 0.05 mol Pi/(mol Ez · s) and EP is 0.91 mol EP/mol Ez, which gives $k_{dephos,[Na^+]=2mM} = 0.055\ s^{-1}$, i.e. a value 10 times smaller than that of $k_{dephos,[Na^+]=0}$. Therefore, it can be concluded that the phosphoenzyme formed in the absence of Na^+ is different from the one formed after the binding of three Na^+.

Table 4
Meaning of the coefficients present in the model shown in Fig. 5.

Coefficient	Meaning
f_T	$[E1ATP]/denom_T$
f_{Trb}	$[E1ATPRb^+]/denom_T$
f_{Trb2}	$[E1ATPRb^+_2]/denom_T$
f_{Tna3}	$[E1ATPNa^+_3]/denom_T$
$denom_T$	$[E1ATP] + [E1ATPRb^+] + [E1ATPRb^+_2] + + [E1ATPNa^+] + [E1ATPNa^+_2] + [E1ATPNa^+_3]$
f_X	$[EXP]/denom_X$
f_{Xrb}	$[EXPRb^+]/denom_X$
$denom_X$	$[EXP] + [EXPNa^+] + [EXPRb^+]$
f_N	$[ENP]/denom_N$
f_{Nna}	$[ENPNa^+]/denom_N$
f_{Nna2}	$[ENPNa^+_2]/denom_N$
$denom_N$	$[ENP] + [ENPNa^+] + [ENPNa^+_2]$

Table 5
Best global fitting values for the parameters of the model presented in Fig. 5. SE values were omitted as they were higher than the values of their corresponding parameters. High values of SE are expected to occur due to a high correlation between the parameters of the model.

Parameter	Value	Units
k_{occ}	500[a]	s^{-1}
k_{deocc}	10.53[b]	s^{-1}
k_{2na3}	200[a]	s^{-1}
k_2	0.310	s^{-1}
k_{2rb}	0.251	s^{-1}
k_{4X}	1.09	s^{-1}
k_{4Xrb}	9.72	s^{-1}
k_{5X}	0.259	s^{-1}
k_{5Xrb}	5.30	s^{-1}
k_{4N}	0.0459	s^{-1}
k_{4Nna}	1.78	s^{-1}
k_{4Nna2}	4.45	s^{-1}
k_{5Nna2}	3.79	s^{-1}
K_{T10}	0.255	mM
K_{T20}	0.469	mM
K_{T30}	482	mM
K_{T01}	0.746	mM
K_{T02}	138	mM
K_{X10}	0.522	mM
K_{X01}	0.0194	mM
K_{N10}	979	mM
K_{N20}	99	mM

[a] Fixed according to values proposed by Heyse et al. [37].
[b] Measured in our laboratory (SE = 0.43 s^{-1}).

3.3. A minimal model

Fig. 5 shows a minimal model that adequately describes the results (see continuous lines in Fig. 7; best fitting values for the parameters are listed in Table 5). Reaction intermediates within a rapid equilibrium segment are grouped (see [19]) and included into a box. Intermediates within each box are explicitly shown in Fig. 6, and their fractional concentrations, f_i, are defined in Table 4. The steady-state levels of states E1 and E2(Rb^+_2) with no ATP bound were considered to be negligible because of the saturating ATP concentrations employed in the determinations. Enzyme phosphorylation and dephosphorylation were considered irreversible due to the absence of ADP and Pi, respectively, in the reaction media. As the distinction between E1P and E2P is not required for reproducing the results, these species were lumped together into a single entity, ENP, i.e. E1P + E2P. ENP represents the phosphoenzyme formed upon the binding of three Na^+ ions to E1ATP.

According to the model:

- When Na^+ and Rb^+ are absent, the X/X-ATPasic cycling mode involves the formation of a phosphorylated intermediate different from ENP that we designate as EXP.
- Small increments in $[Rb^+]$ give rise to the X/Rb^+-ATPasic cycling mode, which involves the formation of the occluded-Rb^+ intermediate EX(Rb^+).
- Higher $[Rb^+]$ inhibits ATPase activity with occlusion of Rb^+ through the direct route, leading to an increasing accumulation of E2(Rb^+_2) ATP.
- On the other hand, small increments in $[Na^+]$ inhibit the X/X-ATPase activity by lowering the rate of EXP formation. This effect is mainly exerted by the high affinity binding of one or two Na^+ to E1ATP (lowering f_T, see Table 4 and Fig. 6).
- Na^+ also inhibits EXP dephosphorylation with high affinity (by lowering f_X, see Table 4 and Fig. 6), in such a way that EXP levels

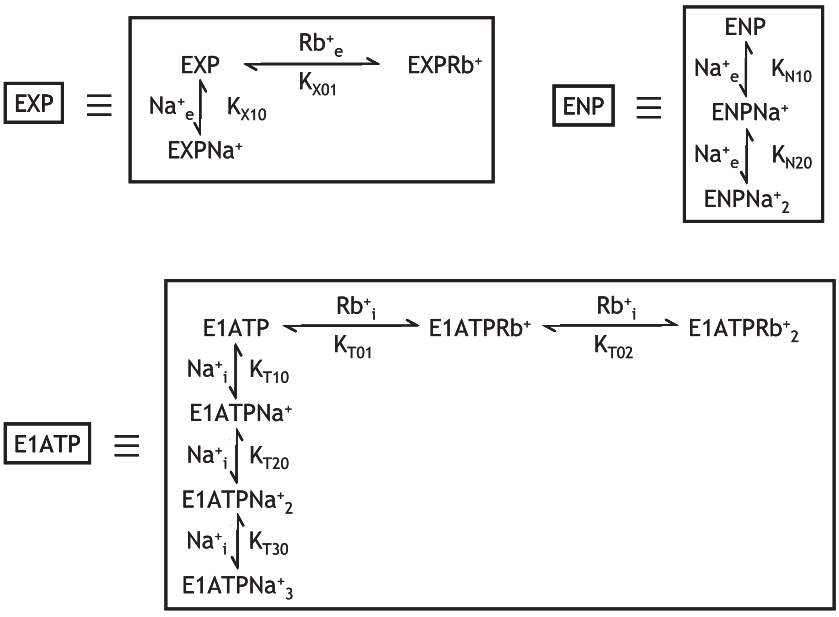

Fig. 6. Intermediates considered in the rapid equilibrium segments. K_i's are apparent equilibrium constants. Intermediates with sodium and rubidium simultaneously bound were not considered because they cannot be formed under the experimental conditions tested.

do not change significantly with [Na^+] below 0.15 mM.

- Higher [Na^+] lead to the fast formation of ENP upon the simultaneous binding of the three transported Na^+ to E1ATP. Although the enzyme rate of phosphorylation is significantly increased, ENP spontaneous rate of dephosphorylation is very low, as well as the ATPase activity.
- The low affinity binding of two Na^+ to ENP (mimicking K^+), increases its rate of dephosphorylation leading to an increase in ATPase activity and a mild decrease in EP levels.

The model shown in Fig. 5 gives the following rational functions of [Na^+] and [Rb^+]:

$$v_{\mathrm{MODEL}}\left(\left[Rb^+\right]\right)=\frac{\alpha_{Rb0}+\alpha_{\mathrm{Rb1}}\cdot\frac{[Rb^+]}{\kappa_{\mathrm{Rb1}}}+\alpha_{Rb2}\cdot\frac{[Rb^+]^2}{\kappa_{\mathrm{Rb1}}\cdot\kappa_{\mathrm{Rb2}}}}{1+\frac{[Rb^+]}{\kappa_{\mathrm{Rb1}}}+\frac{[Rb^+]^2}{\kappa_{\mathrm{Rb1}}\cdot\kappa_{\mathrm{Rb2}}}+\frac{[Rb^+]^3}{\kappa_{\mathrm{Rb1}}\cdot\kappa_{\mathrm{Rb2}}\cdot\kappa_{\mathrm{Rb3}}}} \tag{8}$$

$$Occ_{\mathrm{MODEL}}\left(\left[Rb^+\right]\right)=\frac{\Omega_{\mathrm{Rb1}}\cdot\frac{[Rb^+]}{\kappa_{\mathrm{Rb1}}}+\Omega_{Rb2}\cdot\frac{[Rb^+]^2}{\kappa_{\mathrm{Rb1}}\cdot\kappa_{\mathrm{Rb2}}}+\Omega_{Rb3}\cdot\frac{[Rb^+]^3}{\kappa_{\mathrm{Rb1}}\cdot\kappa_{\mathrm{Rb2}}\cdot\kappa_{\mathrm{Rb3}}}}{1+\frac{[Rb^+]}{\kappa_{\mathrm{Rb1}}}+\frac{[Rb^+]^2}{\kappa_{\mathrm{Rb1}}\cdot\kappa_{\mathrm{Rb2}}}+\frac{[Rb^+]^3}{\kappa_{\mathrm{Rb1}}\cdot\kappa_{\mathrm{Rb2}}\cdot\kappa_{\mathrm{Rb3}}}} \tag{9}$$

$$v_{\mathrm{MODEL}}\left(\left[Na^+\right]\right)=\frac{\begin{array}{l}\alpha_{Na0}+\alpha_{Na1}\cdot\frac{[Na^+]}{\kappa_{\mathrm{Na1}}}+\alpha_{Na2}\cdot\frac{[Na^+]^2}{\kappa_{\mathrm{Na1}}\cdot\kappa_{\mathrm{Na2}}}+\alpha_{Na3}\cdot\frac{[Na^+]^3}{\kappa_{\mathrm{Na1}}\cdot\kappa_{\mathrm{Na2}}\cdot\kappa_{\mathrm{Na3}}}+\\ +\alpha_{\mathrm{Na4}}\cdot\frac{[Na^+]^4}{\kappa_{\mathrm{Na1}}\cdot\kappa_{\mathrm{Na2}}\cdot\kappa_{\mathrm{Na3}}\cdot\kappa_{\mathrm{Na4}}}+\alpha_{Na5}\cdot\frac{[Na^+]^5}{\kappa_{\mathrm{Na1}}\cdot\kappa_{\mathrm{Na2}}\cdot\kappa_{\mathrm{Na3}}\cdot\kappa_{\mathrm{Na4}}\cdot\kappa_{\mathrm{Na5}}}\end{array}}{\begin{array}{l}1+\frac{[Na^+]}{\kappa_{\mathrm{Na1}}}+\frac{[Na^+]^2}{\kappa_{\mathrm{Na1}}\cdot\kappa_{\mathrm{Na2}}}+\frac{[Na^+]^3}{\kappa_{\mathrm{Na1}}\cdot\kappa_{\mathrm{Na2}}\cdot\kappa_{\mathrm{Na3}}}+\\ +\frac{[Na^+]^4}{\kappa_{\mathrm{Na1}}\cdot\kappa_{\mathrm{Na2}}\cdot\kappa_{\mathrm{Na3}}\cdot\kappa_{\mathrm{Na4}}}+\frac{[Na^+]^5}{\kappa_{\mathrm{Na1}}\cdot\kappa_{\mathrm{Na2}}\cdot\kappa_{\mathrm{Na3}}\cdot\kappa_{\mathrm{Na4}}\cdot\kappa_{\mathrm{Na5}}}\end{array}} \tag{10}$$

$$EP_{\mathrm{MODEL}}\left(\left[Na^+\right]\right)=\frac{\begin{array}{l}\varepsilon_{\mathrm{Na0}}+\varepsilon_{\mathrm{Na1}}\cdot\frac{[Na^+]}{\kappa_{\mathrm{Na1}}}+\varepsilon_{\mathrm{Na2}}\cdot\frac{[Na^+]^2}{\kappa_{\mathrm{Na1}}\cdot\kappa_{\mathrm{Na2}}}+\varepsilon_{Na3}\cdot\frac{[Na^+]^3}{\kappa_{\mathrm{Na1}}\cdot\kappa_{\mathrm{Na2}}\cdot\kappa_{\mathrm{Na3}}}+\\ +\varepsilon_{Na4}\cdot\frac{[Na^+]^4}{\kappa_{\mathrm{Na1}}\cdot\kappa_{\mathrm{Na2}}\cdot\kappa_{\mathrm{Na3}}\cdot\kappa_{\mathrm{Na4}}}+\varepsilon_{Na5}\cdot\frac{[Na^+]^5}{\kappa_{\mathrm{Na1}}\cdot\kappa_{\mathrm{Na2}}\cdot\kappa_{\mathrm{Na3}}\cdot\kappa_{\mathrm{Na4}}\cdot\kappa_{\mathrm{Na5}}}\end{array}}{\begin{array}{l}1+\frac{[Na^+]}{\kappa_{\mathrm{Na1}}}+\frac{[Na^+]^2}{\kappa_{\mathrm{Na1}}\cdot\kappa_{\mathrm{Na2}}}+\frac{[Na^+]^3}{\kappa_{\mathrm{Na1}}\cdot\kappa_{\mathrm{Na2}}\cdot\kappa_{\mathrm{Na3}}}+\\ +\frac{[Na^+]^4}{\kappa_{\mathrm{Na1}}\cdot\kappa_{\mathrm{Na2}}\cdot\kappa_{\mathrm{Na3}}\cdot\kappa_{\mathrm{Na4}}}+\frac{[Na^+]^5}{\kappa_{\mathrm{Na1}}\cdot\kappa_{\mathrm{Na2}}\cdot\kappa_{\mathrm{Na3}}\cdot\kappa_{\mathrm{Na4}}\cdot\kappa_{\mathrm{Na5}}}\end{array}} \tag{11}$$

The meaning of the coefficients present in model equations is given in the supplementary material (Tables A and B) and their values are listed in Tables 6 and 7.

According to the model, the coefficients α_{Na0} (which is identical to α_{Rb0}) and $\varepsilon_{\mathrm{Na0}}$ are exclusively given by the X/X-ATPasic cycling mode.

Empirical equations that describe the results obtained as a function of [Rb^+] in the absence of Na^+ (Eqs. (3) and (4)) contain the same polynomial terms as those present in the model equations (Eqs. (8) and (9)). The coefficients α_{Rb1} and Ω_{Rb1} account for the high-affinity increase observed in both ATPase activity and occluded-Rb^+ levels, respectively. They mainly express the cycling mode where the intermediate E1ATP is converted into EXP, which regenerates E1ATP after the binding and occlusion of Rb^+. In addition, the model poses that the binding of one Rb^+ to E1ATP, with low apparent affinity, does

Table 6
Values of the coefficients in model Eqs. (8) and (9) calculated according to Table A (supplementary material) from the best global fitting values in Table 5.

Parameter	Value ± SE	Units
Ω_{Rb1}	0.0533 ± 0.0015	mol Rb^+/mol Ez
Ω_{Rb2}	0.045 ± 0.020	mol Rb^+/mol Ez
Ω_{Rb3}	1.961 ± 0.096	mol Rb^+/mol Ez
κ_{Rb1}	0.00492 ± 0.00026	mM
κ_{Rb2}	0.76 ± 0.18	mM
κ_{Rb3}	2.91 ± 0.38	mM
α_{Rb0}	0.125 ± 0.021	mol Pi/(mol Ez · s)
α_{Rb1}	0.283 ± 0.022	mol Pi/(mol Ez · s)
α_{Rb2}	0.233 ± 0.034	mol Pi/(mol Ez · s)

Table 7
Values of the coefficients in model Eqs. (10) and (11) calculated according to Table B (supplementary material) from the best global fitting values in Table 5. When omitted, SE was higher than its parameter value. High values of SE are expected to occur due to a high correlation between parameters.

Parameter	Value ± SE	Units
ε_{Na0}	0.115 ± 0.019	mol EP/mol Ez
ε_{Na1}	0.12	mol EP/mol Ez
ε_{Na2}	0.0026	mol EP/mol Ez
ε_{Na3}	0.995 ± 0.050	mol EP/mol Ez
ε_{Na4}	0.90	mol EP/mol Ez
ε_{Na5}	0.45	mol EP/mol Ez
κ_{Na1}	0.54	mM
κ_{Na2}	0.53	mM
κ_{Na3}	0.11	mM
κ_{Na4}	880	mM
κ_{Na5}	50	mM
α_{Na0}	0.125 ± 0.038	mol Pi/(mol Ez · s)
α_{Na1}	0.0027	mol Pi/(mol Ez · s)
α_{Na2}	0.000036	mol Pi/(mol Ez · s)
α_{Na3}	0.046	mol Pi/(mol Ez · s)
α_{Na4}	1.6	mol Pi/(mol Ez · s)
α_{Na5}	2.0	mol Pi/(mol Ez · s)

not prevent the formation of EXP. Otherwise, a significant lack of fit of the model would be observed, as can be seen with dashed lines in Fig. 7, panels A and B. It is worth noting that the term containing $[Rb^+]^2$ in numerator of $v_{MODEL}([Rb^+])$ in Eq. (8) is given by these effects of Rb^+ upon its binding to EXP and E1ATP.

For reproducing the results obtained as a function of $[Na^+]$ in the absence of Rb^+, the model poses that the binding of one or two Na^+ to E1ATP and one Na^+ to EXP prevents both, enzyme phosphorylation and dephosphorylation. This makes negligible the coefficients α_{Na1}, α_{Na2}, and α_{Na3} in Eq. (10) (see Table 7), and explains the decrease in ATPase activity observed at low $[Na^+]$. In particular, coefficients α_{Na1} and α_{Na2} are so close to zero, that fitting of the empirical equation describing ATPase activity as a function of $[Na^+]$ (Eq. (6)) is better achieved by setting $a_{Na1} = a_{Na2} = 0$. This effect of Na^+ on EXP and E1ATP also requires the values of coefficients ε_{Na0} and ε_{Na1} in Eq. (11) to be very similar to each other (Table 7), in such a way that the predicted levels of EP show just a slight increase with $[Na^+]$ ranging from 0 to 0.2 mM. This is in agreement with the best empirical fit (Eq. (7)), where e_{Na0}, e_{Na1}, and e_{Na2} in Table 3 have identical values.

Full occupation of the three intracellular Na^+ binding sites (intermediate $E1ATPNa^+_3$) greatly promotes enzyme phosphorylation (giving rise to ENP) but is not enough for increasing ATPase activity because the rate of spontaneous dephosphorylation of ENP is very low, leading to a near maximum value of ε_{Na3} (see Table 7, and Fig. 7 panels C and D) and a value of α_{Na3} lower than that corresponding to α_{Na0}.

It was shown by Beaugé [34] that the rate of enzyme dephosphorylation exhibits a high-affinity decrease and a low-affinity increase with $[Na^+]$. He suggested that the rate of dephosphorylation of E2P (see Fig. 1) is inhibited by the binding of a single Na^+_e with high affinity and stimulated by the binding of a second Na^+_e with low affinity. In his view, the binding of Na^+ takes place at external sites in ENP. An interesting simulation analysis of this possibility and of its consequences on some partial reactions of the pump was carried out by Pedemonte [38]. However, although this assumption roughly reproduces the results (dotted lines in Fig. 7), a considerably better fit is obtained by posing that these effects of Na^+_e take place at

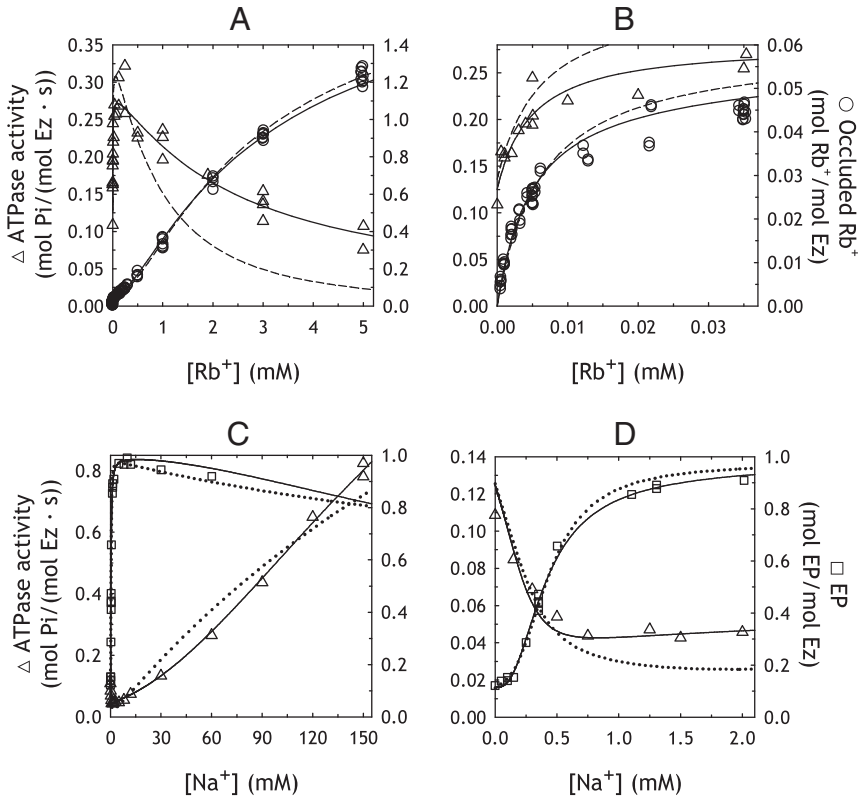

Fig. 7. Fit of models to the results. The continuous lines are the plot of the equations corresponding to the model in Fig. 5 for the best fitting values of the parameters in Table 5. The dashed lines are the plot of the best fit when the parameter k_{2rb} is made equal to zero. The dotted lines are the plot of the best fit when ENP dephosphorylation is inhibited by the high-affinity binding of one Na^+.

different phosphoenzyme forms. At [Na^+] lower than 0.25 mM, most of the phosphoenzyme formed is EXP, and the decrease in the dephosphorylation rate is attributable to the inhibition of its spontaneous dephosphorylation by the high-affinity binding of one Na^+ to this intermediate. At [Na^+] higher than 1 mM, most of the phosphoenzyme formed is ENP, which has two cation binding sites both with very low affinity for Na^+_e. The increase in ATPase activity observed at [Na^+] higher than 10 mM is mainly attributable to the stimulation of enzyme dephosphorylation by the simultaneous binding of two Na^+_e to ENP.

3.4. Final remarks

We have studied the global functioning of Na^+/K^+-ATPase by measuring ATPase activity and the steady-state levels of occluded-Rb^+ and EP intermediates. We tested extreme non-physiological conditions to see the extent at which the Albers–Post model applies, and to quantitatively describe the incidence of alternative cycling modes in order to pose a comprehensive kinetic model.

Despite that alternative models have been proposed, the Albers–Post model remains as the reference framework for describing the Na^+/K^+-ATPase reaction cycle. The most distinct alternative model, the "bicyclic" model, was developed by Plesner and Plesner [9,10] as an attempt to explain quantitative inconsistencies found, together with Nørby and Klodos, between the ATPase activity and the rate of breakdown of the phosphorylated intermediates of the enzyme [39]. In their model, Plesner and Plesner had to include an additional "0-ATPase" cycle to explain the ouabain-sensitive ATPase activity observed in the absence of Na^+ [10]. They reported [40] that the 0-ATPase activity has a high affinity for ATP (apparent Km = 0.4 μM) and that it was competitively inhibited by ADP (Ki = 2.4μM) and by K^+ (Ki = 0.9 mM). They show no activation by K^+, in contrast with the activation effects by low Rb^+ concentrations obtained in our experiments. It should be pointed out that in their experiments Plesner and Plesner used an enzyme preparation purified from ox brain, and histidine (30 mM, pH 7.4 at 37 °C) instead of imidazole, and that they made no attempt to keep the ionic strength constant.

To the best of our knowledge, we show here for the first time direct evidence of Rb^+-occlusion due to a cycling mode that takes place in the absence of Na^+. Although it was known that the enzyme becomes phosphorylated in media lacking Na^+ and that buffer imidazole (particularly imidazole-H^+) increases the steady-state levels of phosphoenzyme [32] no information was available of whether this phosphoenzyme could lead to the formation of occluded-Rb^+ intermediates. Fedosova and Esmann [41] found evidence against the possibility that the effects of imidazole-H^+ and other buffer cations are exerted by binding to transport sites and proposed instead the existence of "nucleotide-domain-related" sites, which may be multiple.

From the analysis of our results we can also conclude that the phosphoenzyme formed in the absence of Na^+ and the phosphoenzyme formed with Na^+ dephosphorylate with different rates, strongly suggesting that they are different species.

Finally, our analysis of the best-fitting empirical equations shows that binding of Na^+ to its transport sites during catalysis is either ordered or, if it is at random, it must occur in rapid equilibrium. Although binding of cations to the Na^+/K^+-ATPase is usually considered as taking place in rapid equilibrium, this must be proved since, if this were not the case, the same results could lead to wrong interpretations of the transport mechanism.

Acknowledgements

The present work was supported by Agencia Nacional de Promoción Científica y Tecnológica, Consejo Nacional de Investigaciones Científicas y Técnicas, and University of Buenos Aires, Argentina.

Appendix A. Supplementary data

Supplementary data to this article can be found online at http://dx.doi.org/10.1016/j.bbamem.2013.01.010.

References

[1] V.R. Schack, J.P. Morth, M.S. Toustrup-Jensen, A.N. Anthonisen, P. Nissen, J.P. Andersen, B. Vilsen, Identification and function of a cytoplasmic K^+ site of the Na^+, K^+-ATPase, J. Biol. Chem. 283 (2008) 27982–27990.
[2] T. Shinoda, H. Ogawa, F. Cornelius, C. Toyoshima, Crystal structure of the sodium–potassium pump at 2.4 Å resolution, Nature 459 (2009) 446–450.
[3] I.M. Glynn, in: A.N. Martonosi (Ed.), The Enzymes of Biological Membranes, 2nd ed., Plenum Press, New York, 1985, pp. 35–114.
[4] I.M. Glynn, Annual review prize lecture "All hands to the sodium pump", J. Physiol. (Lond.) 462 (1993) 1–30.
[5] J.C. Skou, M. Esmann, The Na, K-ATPase, J. Bioenerg. Biomembr. 24 (1992) 249–261.
[6] P.J. Garrahan, I.M. Glynn, Factors affecting the relative magnitudes of the sodium:potassium and sodium:sodium exchanges catalysed by the sodium pump, J. Physiol. 192 (1967) 189–216.
[7] M. Fujita, K. Nagano, N. Mizuno, Y. Tashima, T. Nakao, Ouabain-sensitive Mg^{++}-ATPase, K^+-ATPase and Na^+-ATPase activities accompanying a highly specific Na^+-K^+-ATPase preparation, J. Biochem. 61 (1967) 473–477.
[8] S.J. Karlish, I.M. Glynn, An uncoupled efflux of sodium ions from human red cells, probably associated with Na-dependent ATPase activity, Ann. N. Y. Acad. Sci. 242 (1974) 461–470.
[9] L. Plesner, I.W. Plesner, Kinetics of Na^+-ATPase: influence of Na^+ and K^+ on substrate binding and hydrolysis, Biochim. Biophys. Acta 818 (1985) 222–234.
[10] I.W. Plesner, L. Plesner, Kinetics of ($Na^+ + K^+$)-ATPase: analysis of the influence of Na^+ and K^+ by steady-state kinetics, Biochim. Biophys. Acta 818 (1985) 235–250.
[11] C. Polvani, R. Blostein, Protons as substitutes for sodium and potassium in the sodium pump reaction, J. Biol. Chem. 263 (1988) 16757–16763.
[12] K.H. Lee, R. Blostein, Red cell sodium fluxes catalysed by the sodium pump in the absence of K^+ and ADP, Nature 285 (1980) 338–339.
[13] R. Blostein, Proton-activated rubidium transport catalyzed by the sodium pump, J. Biol. Chem. 260 (1985) 829–833.
[14] Y. Hara, M. Nakao, ATP-dependent proton uptake by proteoliposomes reconstituted with purified Na^+, K^+-ATPase, J. Biol. Chem. 261 (1986) 12655–12658.
[15] Y. Hara, J. Yamada, M. Nakao, Proton transport catalyzed by the sodium pump Ouabain-sensitive ATPase activity and the phosphorylation of Na, K-ATPase in the absence of sodium ions, J. Biochem. 99 (1986) 531–539.
[16] E.L. King, C. Altman, A schematic method of deriving the rate laws for enzyme-catalyzed reactions, J. Phys. Chem. 60 (1956) 1375–1378.
[17] J.T. Wong, C.S. Hanes, Kinetic formulations for enzymic reactions involving two substrates, Can. J. Biochem. Physiol. 40 (1962) 763–804.
[18] W.W. Cleland, Partition analysis and the concept of net rate constants as tools in enzyme kinetics, Biochemistry 14 (1975) 3220–3224.
[19] S. Cha, A simple method for derivation of rate equations for enzyme-catalyzed reactions under the rapid equilibrium assumption or combined assumptions of equilibrium and steady state, J. Biol. Chem. 243 (1968) 820–825.
[20] I. Klodos, M. Esmann, R.L. Post, Large-scale preparation of sodium-potassium ATPase from kidney outer medulla, Kidney Int. 62 (2002) 2097–2100.
[21] P.J. Schwarzbaum, S.B. Kaufman, R.C. Rossi, P.J. Garrahan, An unexpected effect of ATP on the ratio between activity and phosphoenzyme level of Na^+/K^+-ATPase in steady state, Biochim. Biophys. Acta 1233 (1995) 33–40.
[22] R.C. Rossi, S.B. Kaufman, R.M. González Lebrero, J.G. Nørby, P.J. Garrahan, An attachment for nondestructive, fast quenching of samples in rapid-mixing experiments, Anal. Biochem. 270 (1999) 276–285.
[23] K.P. Burnham, D.R. Anderson, Model selection and multimodel inference: a practical information-theoretic approach, Springer, New York, 2002.
[24] S.B. Kaufman, R.M. González-Lebrero, P.J. Schwarzbaum, J.G. Nørby, P.J. Garrahan, R.C. Rossi, Are the states that occlude rubidium obligatory intermediates of the Na^+/K^+-ATPase reaction? J. Biol. Chem. 274 (1999) 20779–20790.
[25] H. Poulsen, H. Khandelia, J.P. Morth, M. Bublitz, O.G. Mouritsen, J. Egebjerg, P. Nissen, Neurological disease mutations compromise a C-terminal ion pathway in the Na^+/K^+-ATPase, Nature 467 (2010) 99–102.
[26] H. Yu, I. Ratheal, P. Artigas, B. Roux, Protonation of key acidic residues is critical for the K^+-selectivity of the Na/K pump, Nat. Struct. Mol. Biol. 18 (2011) 1159–1163.
[27] B. Forbush, Rapid release of ^{42}K and ^{86}Rb from an occluded state of the Na, K-pump in the presence of ATP or ADP, J. Biol. Chem. 262 (1987) 11104–11115.
[28] R.C. Rossi, J.G. Nørby, Kinetics of K^+-stimulated dephosphorylation and simultaneous K^+ occlusion by Na, K-ATPase, studied with the K^+ congener Tl^+. The possibility of differences between the first turnover and steady state, J. Biol. Chem. 268 (1993) 12579–12590.
[29] R.M. Gonzalez-Lebrero, S.B. Kaufman, P.J. Garrahan, R.C. Rossi, The occlusion of Rb^+ in the Na^+/K^+-ATPase II The effects of Rb^+, Na^+, Mg^{2+}, or ATP on the equilibrium between free and occluded Rb^+, J. Biol. Chem. 277 (2002) 5922–5928.
[30] R.D. Peluffo, R.C. Rossi, P.J. Garrahan, A.F. Rega, Low affinity acceleration of the phosphorylation reaction of the Na, K-ATPase by ATP, J. Biol. Chem. 269 (1994) 1051–1056.
[31] S. Mårdh, O. Zetterqvist, Phosphorylation and dephosphorylation reactions of bovine brain (Na^+-K^+)-stimulated ATP phosphohydrolase studied by a rapid mixing technique, Biochim. Biophys. Acta 350 (1974) 473–483.

[32] F.M. Schuurmans Stekhoven, H.G. Swarts, J.J. de Pont, S.L. Bonting, Na^+-like effect of imidazole on the phosphorylation of $(Na^+ + K^+)$-ATPase, Biochim. Biophys. Acta 815 (1985) 16–24.
[33] R.L. Post, C. Hegyvary, S. Kume, Activation by adenosine triphosphate in the phosphorylation kinetics of sodium and potassium ion transport adenosine triphosphatase, J. Biol. Chem. 247 (1972) 6530–6540.
[34] L. Beaugé, Breakdown of Na^+/K^+-exchanging ATPase phosphoenzymes formed from ATP and from inorganic phosphate during Na^+-ATPase activity, Eur. J. Biochem. 268 (2001) 5627–5632.
[35] R. Blostein, Sodium pump-catalyzed sodium–sodium exchange associated with ATP hydrolysis, J. Biol. Chem. 258 (1983) 7948–7953.
[36] I.H. Segel, Enzyme Kinetics: Behavior and Analysis of Rapid Equilibrium and Steady-State Enzyme Systems, Wiley-Interscience, 1975, pp. 646–647.
[37] S. Heyse, I. Wuddel, H.J. Apell, W. Stürmer, Partial reactions of the Na, K-ATPase: determination of rate constants, J. Gen. Physiol. 104 (1994) 197–240.
[38] C.H. Pedemonte, Kinetic mechanism of inhibition of the Na^+-pump and some of its partial reactions by external Na^+ (Na^+_o), J. Theor. Biol. 134 (1988) 165–182.
[39] I.W. Plesner, L. Plesner, J.G. Nørby, I. Klodos, The steady-state kinetic mechanism of ATP hydrolysis catalyzed by membrane-bound $(Na^+ + K^+)$-ATPase from ox brain. III. A minimal model, Biochim. Biophys. Acta 643 (1981) 483–494.
[40] L. Plesner, I.W. Plesner, Ouabain-inhibited ATPase activity in the absence of Na^+ and K^+, in: I.M. Glynn, C. Ellory (Eds.), The Sodium Pump, Proceedings of the 4th International Conference on the Na,K-ATPase, The Company of Biologists Ltd., 1985, pp. 469–474.
[41] N.U. Fedosova, M. Esmann, Nucleotide-binding kinetics of Na, K-ATPase: cation dependence, Biochemistry 43 (2004) 4212–4218.